JPEDAV (2009) 30:334–344
DOI: 10.1007/s11669-009-9557-3
1547-7037 ©ASM International

Computational Study of Mobilities and Diffusivities in bcc Ti-Zr and bcc Ti-Mo Alloys

Yajun Liu, Lijun Zhang, and Di Yu

(Submitted December 14, 2008; in revised form April 5, 2009)

Based on the abundant experimental diffusion data and the thermodynamic parameters in the literature, the atomic mobilities of bcc Ti-Zr and bcc Ti-Mo alloys are critically assessed by means of the CALPHAD technique in this work. Comprehensive comparisons between the calculated and experimentally measured diffusion coefficients are made, where the presently obtained mobility parameters can satisfactorily reproduce most of the experimental data. Moreover, the atomic mobilities derived in the present work are successfully applied to reproduce some measured concentration profiles from diffusion couples in both binary systems and the displacements of Kirkendall makers in the Ti-Mo binary system. It is believed that the proposed atomic mobility parameters contribute to the establishment of a general Ti mobility database, which is useful in designing novel high-temperature Ti alloys.

Keywords bcc, CALPHAD, diffusion, mobility, Ti-Zr, Ti-Mo

1. Introduction

Because of the attractive combination of high specific strength, high modulus, low thermal expansion, good fatigue strength, and good corrosion resistance, Ti alloys can provide ideal engineering properties over a wide temperature range up to about 823 K for lighter and stronger structures in aerospace industries.[1] In addition, Ti, Zr, and Mo have been identified as non-toxic elements by tissue-reaction studies, as they show no adverse effect in human body.[2-4] As such, Ti alloys containing Zr and Mo are desirable biomedical alloys in that their biological and physical properties play an important role in the longevity of prostheses and implants.

Knowledge of both thermodynamic and kinetic characteristics of Ti alloys is of critical importance in understanding how temperature, time, and compositions affect alloy microstructures in heat treatment.[5] Such information is not only useful to determine alloy stability under long-term service conditions but also valuable in dealing with processing designs. Inspired by the CALPHAD (CALculation of PHAse Diagram) method, Andersson and Ågren[6] suggested a similar procedure to represent the atomic mobilities of individual species in a multicomponent solution phase. The activation enthalpy term and the logarithm frequency term are expanded by the Redlick-Kister polynomials, which provide a convenience means of advancing into higher order systems from the mobility parameters assessed for unary and binary systems. Such a treatment can provide an in-depth evaluation of various experimental measurements from various authors and give a satisfactory confidence on the parameter quality, thereby becoming a popular means in alloy design. The atomic mobilities are pure kinetic quantities and are therefore independent of thermodynamics. However, combined with thermodynamic information, intrinsic diffusion coefficients and interdiffusion coefficients can be uniquely calculated to simulate problems of interest. In addition, mobilities have advantages over diffusivities in that the number of parameters required for a general diffusion database can be greatly reduced.

Although a general atomic mobility database was developed for fcc Ni super-alloys,[7] there have been very limited works reported for atomic mobilities in bcc Ti high-temperature alloys.[8-10] The aim of this work is to evaluate the atomic mobilities in bcc Ti-Zr and bcc Ti-Mo alloys. The proposed atomic mobilities will be combined into a general bcc Ti mobility database being constructed, which can provide detailed information on diffusion characteristics of bcc Ti alloys.

2. Model Description

Determination of mobility parameters requires various experimental diffusion coefficients, i.e., tracer diffusion coefficients, intrinsic diffusion coefficients, and interdiffusion coefficients. Tracer diffusion coefficients are generally determined from diffusion studies using isotopes. Intrinsic diffusion coefficients are measured with inert markers.

Yajun Liu, Western Transportation Institute, Montana State University, Bozeman, MT 59715, USA; **Lijun Zhang**, State Key Laboratory of Powder Metallurgy, Central South University, Changsha, Hunan 410083, People's Republic of China; **Di Yu**, American Water Chemicals Inc., Tampa, FL 33619, USA. Contact e-mail: pcbook@hotmail.com and yajunliu@gatech.edu.

Interdiffusion coefficients are obtained in the number-fixed frame of reference from concentration profiles using diffusion couples. In what follows, we will discuss a general fictitious A-B binary system to demonstrate the inherent relations between various diffusion coefficients.

In the lattice reference frame, the diffusion flux of element A is given by[11]:

$$J_{\mathrm{A}}^{\mathrm{I}} = -C_{\mathrm{A}} M_{\mathrm{A}} \frac{\partial \mu_{\mathrm{A}}}{\partial x} \quad \text{(Eq 1)}$$

where C_{A} is the volume concentration of A; M_{A} is the atomic mobility of A; μ_{A} is the chemical potential of A; I stands for the intrinsic reference frame.

The diffusion flux of A can also be defined through:

$$J_{\mathrm{A}}^{\mathrm{I}} = -D_{\mathrm{A}}^{\mathrm{I}} \frac{\partial C_{\mathrm{A}}}{\partial x} \quad \text{(Eq 2)}$$

where $D_{\mathrm{A}}^{\mathrm{I}}$ is the intrinsic diffusion coefficient of A.

Equating the two expressions in Eq 1 and 2 results in:

$$-D_{\mathrm{A}}^{\mathrm{I}} \frac{\partial C_{\mathrm{A}}}{\partial x} = -C_{\mathrm{A}} M_{\mathrm{A}} \frac{\partial \mu_{\mathrm{A}}}{\partial x} \quad \text{(Eq 3)}$$

The chemical potential gradient can be evaluated with the concentration gradients by:

$$\frac{\partial \mu_{\mathrm{A}}}{\partial x} = \frac{\partial \mu_{\mathrm{A}}}{\partial x_{\mathrm{A}}} \frac{\partial x_{\mathrm{A}}}{\partial x} + \frac{\partial \mu_{\mathrm{A}}}{\partial x_{\mathrm{B}}} \frac{\partial x_{\mathrm{B}}}{\partial x} \quad \text{(Eq 4)}$$

where x_{A} and x_{B} are the molar fractions of A and B, respectively.

With the molar volume of the phase being constant, it follows from Eq 3 and 4 that:

$$D_{\mathrm{A}}^{\mathrm{I}} = x_{\mathrm{A}} M_{\mathrm{A}} \left(\frac{\partial \mu_{\mathrm{A}}}{\partial x_{\mathrm{A}}} - \frac{\partial \mu_{\mathrm{A}}}{\partial x_{\mathrm{B}}} \right) \quad \text{(Eq 5)}$$

The chemical potential of component A is given by:

$$\mu_{\mathrm{A}} = G_{\mathrm{m}} + \frac{\partial G_{\mathrm{m}}}{\partial x_{\mathrm{A}}} - x_{\mathrm{A}} \frac{\partial G_{\mathrm{m}}}{\partial x_{\mathrm{A}}} - x_{\mathrm{B}} \frac{\partial G_{\mathrm{m}}}{\partial x_{\mathrm{B}}} \quad \text{(Eq 6)}$$

where $G_{\mathrm{m}}^{\mathrm{bcc}}$ denotes the molar Gibbs free energy of the bcc phase that is described by:

$$G_{\mathrm{m}}^{\mathrm{bcc}} = x_{\mathrm{A}} {}^{0}G_{\mathrm{A}}^{\mathrm{bcc}} + x_{\mathrm{B}} {}^{0}G_{\mathrm{B}}^{\mathrm{bcc}} + RT(x_{\mathrm{A}} \ln x_{\mathrm{A}} + x_{\mathrm{B}} \ln x_{\mathrm{B}}) + {}^{\mathrm{ex}}G_{\mathrm{m}}^{\mathrm{bcc}} \quad \text{(Eq 7)}$$

where ${}^{0}G_{\mathrm{A}}^{\mathrm{bcc}}$ and ${}^{0}G_{\mathrm{B}}^{\mathrm{bcc}}$ are the molar Gibbs free energies of pure bcc A and pure bcc B, respectively; ${}^{\mathrm{ex}}G_{\mathrm{m}}^{\mathrm{bcc}}$ is the excess Gibbs free energy that is expressed by the Redlich-Kister polynomials as below:

$${}^{\mathrm{ex}}G_{\mathrm{m}}^{\mathrm{bcc}} = x_{\mathrm{A}} x_{\mathrm{B}} \sum_{i} {}^{i}L_{\mathrm{A,B}} (x_{\mathrm{A}} - x_{\mathrm{B}})^{i} \quad \text{(Eq 8)}$$

The combination of Eq 5 and 6 leads to:

$$D_{\mathrm{A}}^{\mathrm{I}} = x_{\mathrm{A}} x_{\mathrm{B}} M_{\mathrm{A}} \left(\frac{\partial^2 G_{\mathrm{m}}}{\partial x_{\mathrm{A}}^2} + \frac{\partial^2 G_{\mathrm{m}}}{\partial x_{\mathrm{B}}^2} - 2\frac{\partial^2 G_{\mathrm{m}}}{\partial x_{\mathrm{A}} \partial x_{\mathrm{B}}} \right) \quad \text{(Eq 9)}$$

Similarly, the intrinsic diffusion coefficient of B can be obtained as:

$$D_{\mathrm{B}}^{\mathrm{I}} = x_{\mathrm{A}} x_{\mathrm{B}} M_{\mathrm{B}} \left(\frac{\partial^2 G_{\mathrm{m}}}{\partial x_{\mathrm{A}}^2} + \frac{\partial^2 G_{\mathrm{m}}}{\partial x_{\mathrm{B}}^2} - 2\frac{\partial^2 G_{\mathrm{m}}}{\partial x_{\mathrm{A}} \partial x_{\mathrm{B}}} \right) \quad \text{(Eq 10)}$$

The tracer diffusion coefficients of A and B (denoted by D_{A}^{*} and D_{B}^{*}, respectively) can be related to their mobilities by:

$$D_{\mathrm{A}}^{*} = RTM_{\mathrm{A}} \quad \text{(Eq 11)}$$

$$D_{\mathrm{B}}^{*} = RTM_{\mathrm{B}} \quad \text{(Eq 12)}$$

where R is the gas constant; T is the temperature.

According to the absolute rate theory, the mobility for element i (i = A or B) can be divided into a frequency factor, M_i^0, and an activation enthalpy, Q_i, by[12,13]:

$$M_i = \frac{1}{RT} \exp\left(\frac{-Q_i + RT \ln(M_i^0)}{RT} \right) = \frac{1}{RT} \exp\left(\frac{\Phi_i}{RT} \right) \quad \text{(Eq 13)}$$

where Φ_i is a composition-dependent property which can be expressed by the Redlick-Kister polynomials as below:

$$\Phi_i = x_{\mathrm{A}} \Phi_i^{\mathrm{A}} + x_{\mathrm{B}} \Phi_i^{\mathrm{B}} + x_{\mathrm{A}} x_{\mathrm{B}} \sum_{r} {}^{r}\Phi_i^{\mathrm{A,B}} (x_{\mathrm{A}} - x_{\mathrm{B}})^{r} \quad \text{(Eq 14)}$$

where Φ_i^{A}, Φ_i^{B}, and ${}^{r}\Phi_i^{\mathrm{A,B}}$ are the model parameters to be evaluated from experimental data in this work.

The temporal and spatial evolution of element i (i = A or B) can be obtained by the following partial differential equation with suitable initial and boundary conditions:

$$\frac{\partial x_i}{\partial t} + \nabla \cdot (-\tilde{D} \nabla x_i) = 0 \quad \text{(Eq 15)}$$

where $\tilde{D}$ is the interdiffusion coefficient defined by[14]:

$$\tilde{D} = (x_{\mathrm{A}} D_{\mathrm{B}}^{\mathrm{I}} + x_{\mathrm{B}} D_{\mathrm{A}}^{\mathrm{I}}) \quad \text{(Eq 16)}$$

In the CALPHAD notation, $\tilde{D} = D_{\mathrm{AA}}^{\mathrm{B}} = D_{\mathrm{BB}}^{\mathrm{A}}$. $D_{\mathrm{AA}}^{\mathrm{B}}$ is the diffusion coefficient relating the flux of A with its own concentration gradient, and $D_{\mathrm{BB}}^{\mathrm{A}}$ has similar meaning.

The thermodynamic parameters for the Ti-Zr and Ti-Mo binary systems are taken from the assessment of Turchanin et al.[15] and Shim et al.,[16] respectively. The mobility parameters for the self-diffusion coefficients of bcc Ti and bcc Zr are taken from our earlier papers on the mobilities of Ti-V[9] and Nb-Zr[17] binary systems, respectively. The assessment of the other mobility parameters is carried out by an iterative optimization based on the minimization of the residuals between the calculated and experimental values in the literature. The detailed optimization process for a binary substitutional solution can be found in Ref 9 and 17, where the method used is essentially the same as that suggested by Campbell.[18] For a similar example on how to implement an inverse problem in Comsol Multiphysics, the readers are referred to Ref 19 for more details. In all computational studies of diffusion annealing that are undertaken to

investigate temporal and spatial evolution within diffusion couples, Eq 15 is solved with the finite element method implemented in Comsol Multiphysics. All the simulations are set up in one-dimensional planar geometries with closed boundary conditions for mass conservation. To get accurate results, 512 evenly distributed Lagrange-quadratic elements are employed and the time steps are automatically controlled by the software.

3. Experimental Information

3.1 The Ti-Zr System

Pavlinov[20] studied the impurity diffusion of Zr in polycrystalline bcc Ti. The diffusion coefficients were determined by the radioactive isotopes of ^{95}Zr with the integral residual method from 1193 to 1773 K. Using Ti/Ti-3.06 at.% Zr diffusion couples, Araki et al.[21] determined the impurity diffusion coefficients of Zr in bcc Ti at temperatures from 1173 to 1773 K under pressures of 0.1 MPa and 1.0, 2.1, and 3.0 GPa. The diffusion couples annealed at various pressures and temperatures were analyzed with an electron probe microanalyzer (EPMA) to determine the penetration profiles, after which the impurity diffusion coefficients of Zr in Ti were determined by the Hall method. Herzig et al.[22] investigated the tracer diffusion coefficients of ^{44}Ti and ^{95}Zr in bcc Ti-Zr alloys with 49 at.% Zr within the whole temperature range of the bcc phase. The Arrhenius plots were strongly curved, which share the same characteristics of self-diffusion in pure bcc Ti and bcc Zr.

Thibon et al.[23] studied the interdiffusion in bcc Ti-Zr alloys from 1103 to 2003 K within the whole composition range. For the temperature from 1273 to 1723 K, diffusion couples were made of pure Ti and Zr. For the other temperatures, pure metals and alloys were used to avoid fusion or phase transformation during diffusion annealing under purified argon. The concentration profiles were obtained by EPMA parallel to the diffusion direction, and the interdiffusion coefficients were calculated by the den Broeder method. The Hall method was used to determine the diffusion coefficients at the Ti-rich and Zr-rich sides. Although the impurity diffusion coefficients in Ti and Zr show the anomalous diffusion behavior, this tendency is not observed for the interdiffusion in the Ti-Zr alloys. Brunsch and Steeb[24] investigated the interdiffusion in the binary Ti-Zr system by Ti/Zr diffusion couples. Diffusion annealing was undertaken from 923 to 1323 K, after which the diffusion couples were characterized by means of EPMA. The interdiffusion coefficients were determined by the Matano method for each temperature through the whole composition range, which show a slight rise with the Ti concentration.

Raghunathan et al.[25] carried out the interdiffusion study in diffusion couples made of Zr and Ti-Zr alloys. The diffusion couples were annealed at 1441, 1363, 1303, 1233, and 1174 K for enough time to form suitable concentration curves for chemical analysis. The interdiffusion coefficients were reported for such temperatures within the whole composition range. The results show that the interdiffusion coefficients generally increase with the Ti content at each temperature, but the composition dependence is weak. Using incremental diffusion couples, Bhanumurthy et al.[26] employed a relatively simple method to study the interdiffusion behavior of bcc Ti-Zr alloys at 1173 K. The Boltzmann-Matano and Hall methods were used to determine the diffusion coefficients and their related composition dependence.

3.2 The Ti-Mo System

Using ^{99}Mo isotopes, Borisov et al.[27] measured the Mo self-diffusion coefficients from 2073 to 2448 K in polycrystalline Mo by residual activity measurement. Bronfin et al.[28] investigated the ^{99}Mo self-diffusion coefficients from 1973 to 2193 K in polycrystalline Mo by mechanical and electrochemical sectioning. Danneberg and Krautz[29] applied ^{99}Mo to measure the Mo self-diffusion coefficients from 2173 to 2353 K in polycrystalline wires by means of electrochemical sectioning in radial direction, where the effects of grain boundary diffusion were observed. Employing ^{99}Mo and mechanical sectioning, Askill and Tomlin[30] reported the Mo self-diffusion coefficients from 2123 to 2618 K in single crystals. With ^{99}Mo, Maier et al.[31] measured the Mo self-diffusion coefficients from 1360 to 2773 K in single crystals by mechanical and sputter sectioning. Using ^{99}Mo, Gruzin et al.[32] determined the self-diffusion coefficients of Mo in polycrystals from 2073 to 2473 K by the residual activity method. Pavlinov and Bykov[33] measured the self-diffusion coefficients of ^{99}Mo in polycrystals from 2428 to 2813 K with the integral residual method.

Pavlinov[20] studied the impurity diffusion coefficients of ^{99}Mo in polycrystalline Ti from 1173 to 1833 K with the residual activity method. Gibbs et al.[34] measured the impurity diffusion coefficients of ^{99}Mo in polycrystalline Ti using the lathe sectioning technique. The annealing temperature ranged from 1173 to 1923 K.

Heumann and Imm[35] measured the interdiffusion coefficients and intrinsic diffusion coefficients with respect to the Mo content in bcc Ti-Mo alloys. Diffusion couples were made of pure Ti and pure Mo, in which the Kirkendall effect was examined by the foil method. The diffusion couples were annealed at 1300-1800 K, and the composition profiles in the diffusion zones were determined by EPMA. The displacements of Kirkendall markers and non-Kirkendall markers at various temperatures were studied. As a result, the intrinsic diffusion coefficients and interdiffusion coefficients were reported for the Ti-rich solutions.

Ti atoms diffuse much faster than Mo atoms, and therefore the concentration curves determined from diffusion couples will show a steep concentration gradient near the Mo-rich edge. Such a geometric property will impose challenges in accurate evaluation of the concentration gradients from which interdiffusion coefficients can be obtained. To overcome this problem, Hartley et al.[36] utilized three kinds of semi-infinite diffusion couples, i.e., Ti/Mo, Ti/Ti-50 at.% Mo and Mo/Ti-50 at.% Mo. The diffusion couples were annealed at 1673 K, after which the

compositions in the diffusion zones were determined by EPMA. The interdiffusion coefficients near the Ti-rich edge determined from two kinds of diffusion couples are very consistent, but there exist significant deviations near the Mo-rich edge.

Thibon et al.[37] investigated the interdiffusion in bcc Ti-Mo alloys by means of Ti/Mo diffusion couples from 1523 to 1873 K, Mo/Ti-25.6 at.% Mo diffusion couples for 2023 K and Mo/Ti-33.9 at.% Mo diffusion couples for 2073 K. The diffusion profiles were obtained by EPMA along the diffusion direction. The interdiffusion coefficients were evaluated by the den Broeder method, which are strongly dependent on the composition. The Hall method was used to evaluate impurity diffusion coefficients at the two concentration limits. Although the Kirkendall effect was studied, the authors did not present any result on the intrinsic diffusion coefficients or marker displacement.

Fedotov et al.[38] studied the mutual diffusion in the Ti-Mo system. After preliminary experiments in mutual diffusion between pure metals, it was found necessary to carry out mutual diffusion between pure Ti and Ti-42 wt.% Mo alloys in order to get a more extensive diffusion layer. The diffusion annealing was performed at 1773, 1623, and 1173 K. The elemental distribution in diffusion zones was determined by local spectral x-ray analysis, and the interdiffusion coefficients were calculated by the Matano method.

Majima and Isomoto[39] investigated the diffusion process in Ti/Mo diffusion couples from 1473 to 1673 K by means of the Boltzmann-Matano method. Kirkendall marker displacements and the concentrations on the Matano plane with respect to time and temperatures were reported. Ti atoms were found to diffuse faster than Mo atoms by a factor of 4. Sprengel et al.[40] carried out interdiffusion experiments in diffusion couples made of Ti-5 at.% Mo and Ti-15 at.% Mo alloys. The concentration distribution after diffusion annealing was measured with EPMA, and the interdiffusion coefficients were determined by the Boltzmann-Matano method. The interdiffusion coefficients were found to be concentration dependent and decrease with the Mo content.

4. Results and Discussion

The task of CALPHAD assessment is to find a compromised solution that can represent most of the reported values from different authors. Tracer diffusion coefficients can be more accurately measured than other types of diffusion coefficients. Interdiffusion coefficients, on the contrary, are prone to operational aspects. In all the assessment, we follow the following procedure to evaluate the data quality from different authors with different methods.

(1) The self-diffusion coefficients and impurity diffusion coefficients are collected and compared. For those data that are significantly different from the others, they are classified as dormant data with a weighting factor of zero. The four mobility end-members can therefore be obtained.

(2) The tracer diffusion coefficients or intrinsic diffusion coefficients are then taken into consideration to evaluate the interaction parameters for each element. If the tracer diffusion coefficients are available for only one element, the interaction parameters for that element will be assessed, and the rest parameters will be evaluated from the intrinsic diffusion coefficients or the interdiffusion coefficients.

(3) The interdiffusion coefficients entail more skills to assign weighting factors. According to Eq 16, the interdiffusion coefficients at extremely small solute concentrations will be equivalent to the corresponding impurity diffusion coefficients. As such, the interdiffusion coefficients for different temperatures from different authors should be extrapolated firstly, after which the obtained impurity diffusion coefficients will be compared with the measured impurity diffusion coefficients collected in Step 1. For these interdiffusion coefficients that have satisfactory extrapolation properties, they should be given the highest weighting factor in the assessment.

(4) The concentration curves are the last to be evaluated, which can be incorporated into the optimization process when reasonable interaction parameters have been obtained in the above steps.

4.1 The Ti-Zr System

The atomic mobilities obtained in this work for bcc Ti-Zr alloys are presented in Table 1, where the published mobility parameters for the self-diffusion coefficients of bcc Ti and bcc Zr are also presented. The calculated Ti-Zr phase diagram according to the thermodynamic assessment of Turchanin et al.[15] is given in Fig. 1. This diagram shows a simple geometry where two congruent transformations are evident. The calculated and experimentally measured impurity diffusion coefficients of Ti in bcc Zr and Zr in bcc Ti are presented in Fig. 2 and 3, respectively, where the logarithm values are plotted against reciprocal temperature. It should be noted that the values from Raghunathan et al.[25] in Fig. 3 are not included in the assessment process because they are extrapolated from interdiffusion coefficients and are not consistent with the results from other works. As is evident, the experimental values on the impurity diffusion coefficients can be well represented with the mobility parameters proposed in this work. The temperature dependence of impurity diffusion coefficients can be described by the Arrhenius expression from the practical point of view. The tracer diffusion coefficients characterize the diffusion rate of an element in response to the corresponding concentration gradients within an ideal solution in the lattice reference frame. The calculated tracer diffusion coefficients of Ti and Zr at 49 at.% Zr are plotted in Fig. 4 and 5, where the experimental data from Herzig et al.[22] are given for comparison. The nonlinear nature in Fig. 5 stems from the mobility parameters for Zr self-diffusion that are described in a piece-wise manner.

The calculated and measured interdiffusion coefficients from Thibon et al.[23] are presented in Fig. 6 against the Ti

Table 1 Mobility parameters for the bcc phase in the Ti-Zr binary system (all in SI units)

Phase	Model	Mobility	Parameters
bcc	$(Ti,Zr)_1(Va)_3$	Ti	$\Phi^{Ti}_{Ti} = -151989.95 - 127.37T$ [9] $\Phi^{Zr}_{Ti} = -140356.54 - 138.12T$ ${}^0\Phi^{Ti,Zr}_{Ti} = -15826.04 + 62.55T$ ${}^1\Phi^{Ti,Zr}_{Ti} = 8243.54$
		Zr	$\Phi^{Zr}_{Zr} = \begin{cases} -104624.81 - 163.15T & T \le 1573\ K \\ -161543.53 - 126.10T & T \ge 1573\ K \end{cases}$ [17] $\Phi^{Ti}_{Zr} = -131670.56 - 133.36T$ ${}^0\Phi^{Ti,Zr}_{Zr} = -12581.03 + 33.38T$ ${}^1\Phi^{Ti,Zr}_{Zr} = 2898.60$

Note: Mobility parameters for self-diffusion of bcc Ti and bcc Zr are taken from Ref 9 and 17, respectively. It should be noted that the thermodynamic parameters for bcc phase and hcp phase in Ref 15 should be exchanged in order to reproduce the correct results

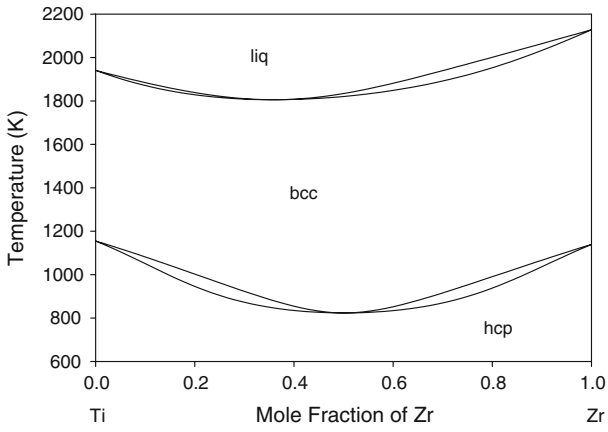

Fig. 1 Calculated Ti-Zr binary phase diagram according to the thermodynamic data of Turchanin et al.[15]

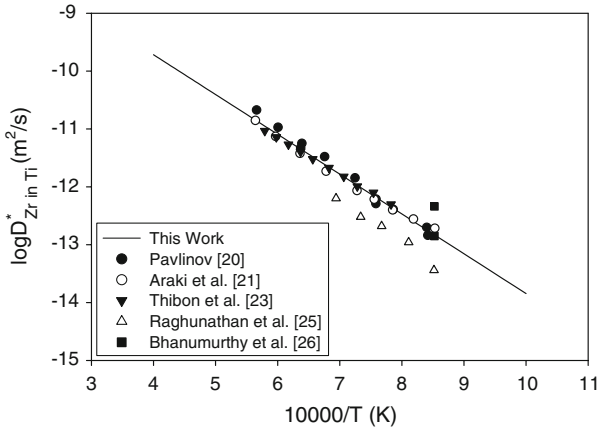

Fig. 3 Calculated and experimentally measured impurity diffusion coefficients of Zr in bcc Ti

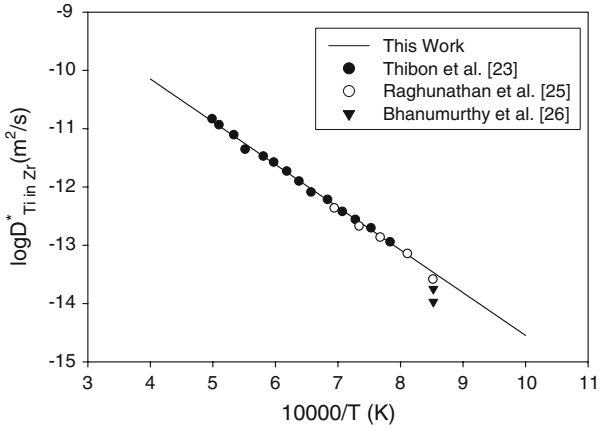

Fig. 2 Calculated and experimentally measured impurity diffusion coefficients of Ti in bcc Zr

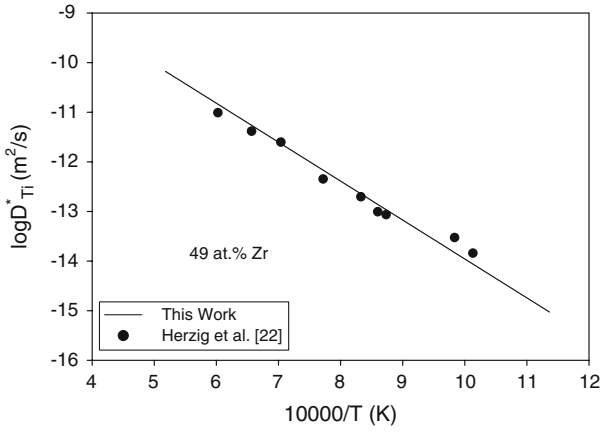

Fig. 4 Calculated and experimentally measured Ti tracer diffusion coefficients in bcc Ti-Zr alloys

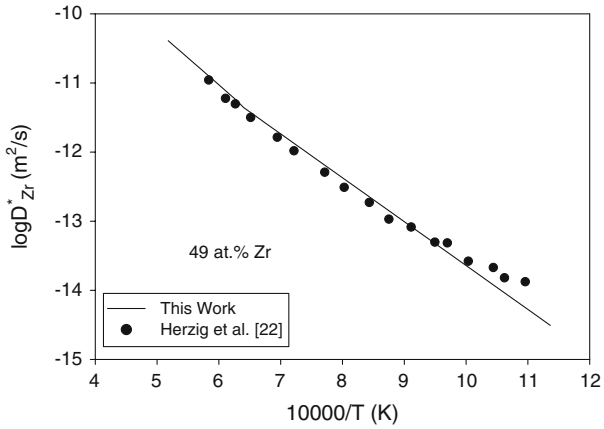

Fig. 5 Calculated and experimentally measured Zr tracer diffusion coefficients in bcc Ti-Zr alloys

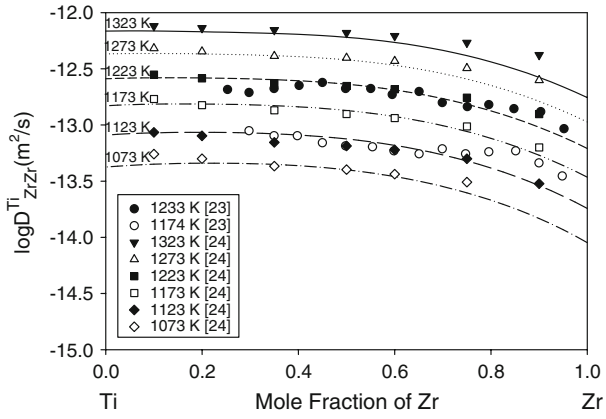

Fig. 7 Calculated and experimentally measured interdiffusion coefficients in bcc Ti-Zr alloys

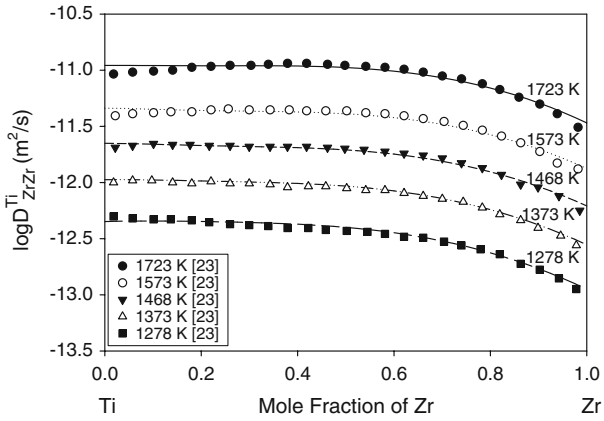

Fig. 6 Calculated and experimentally measured interdiffusion coefficients in bcc Ti-Zr alloys

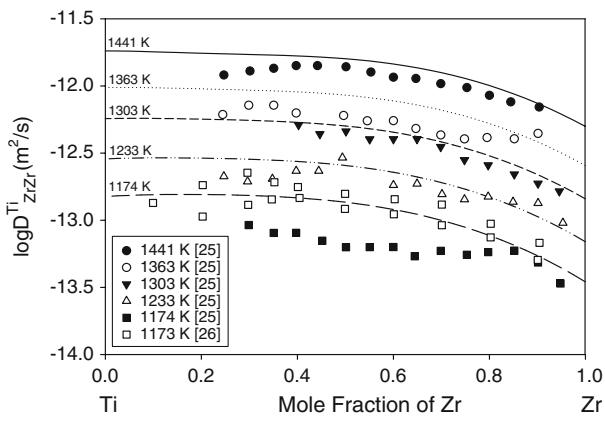

Fig. 8 Calculated and experimentally measured interdiffusion coefficients in bcc Ti-Zr alloys

concentration, where good agreement is evident within the whole composition range. As is evident, the interdiffusion coefficients generally increase with the Ti content, but depend weakly on the concentration, particularly for the Zr content lower than 50 at.%, beyond which a slight decrease is observed when the Zr content increases. The calculated interdiffusion coefficients in bcc Ti-Zr alloys at 1323, 1273, 1223, 1173, 1123, and 1073 K are presented in Fig 7, together with the experimental data reported by Thibon et al.[23] and Brunsch and Steeb.[24] The calculated interdiffusion coefficients are generally in accordance with the experimental data at various temperatures. Figure 8 presents the comparison between the calculated and experimental interdiffusion coefficients from Raghunathan et al.[25] and Bhanumurthy et al.[26] at various temperatures. Although the experimental data are somewhat scattered, those values are generally distributed around the calculated lines, indicating the validity of the mobility parameters proposed in this work.

The interdiffusion coefficients in Fig. 6 can be well extrapolated to obtain both kinds of impurity diffusion coefficients, and therefore all the data points in Fig. 6 are equally treated and given high weighting factors. According to the criteria given above for assessment, the data presented in Fig. 7 have their own problems. As can be seen in Fig. 7, the impurity diffusion coefficient of Zr in bcc Ti at each temperature can be reasonably extrapolated from the interdiffusion coefficients, but such is not the case for the impurity diffusion coefficients of Ti in bcc Zr. The adverse problem is seen in Fig. 8, where the impurity diffusion coefficients of Ti in bcc Zr can be well extrapolated. Higher weighting factors are therefore assigned to the data near the Ti-edge in Fig. 7 and the data near the Zr-edge in Fig. 8.

Figures 9, 10, and 11 present the calculated and experimentally measured elemental distribution in diffusion couples, where the initial alloy configuration, annealing time and temperature are also superimposed. As can be expected, the concentration curves feature an almost symmetric characteristic around the Matano plane, which is typical of interdiffusion coefficients that weakly depend on the composition.

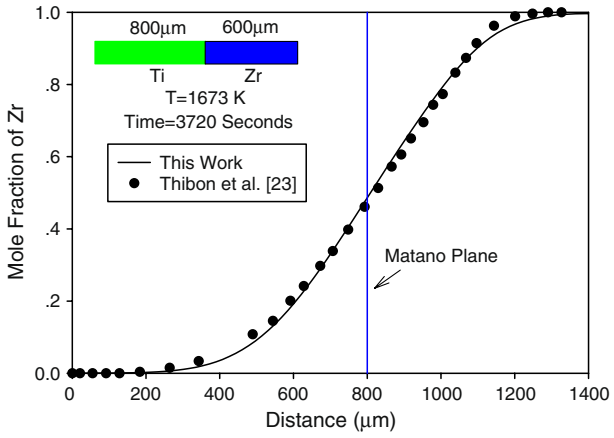

Fig. 9 Calculated and experimentally measured Zr distribution in a Ti/Zr diffusion couple

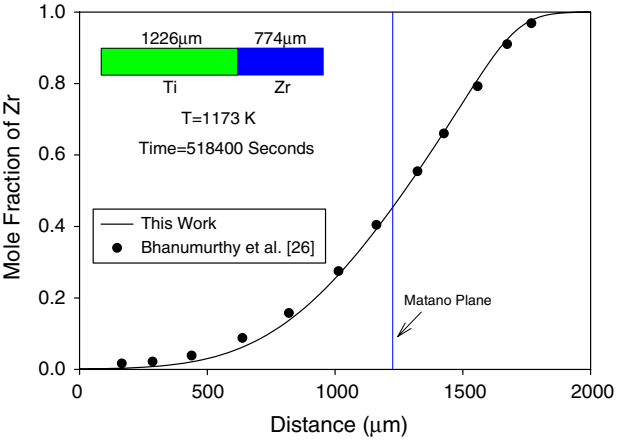

Fig. 10 Calculated and experimentally measured Zr distribution in a Ti/Zr diffusion couple

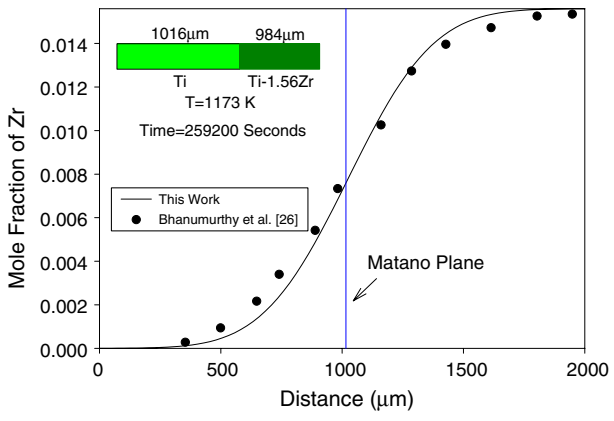

Fig. 11 Calculated and experimentally measured Zr distribution in a Ti/Ti-1.56 at.% Zr diffusion couple

4.2 The Ti-Mo system

The atomic mobilities for bcc Ti-Mo alloys obtained in this work are given in Table 2. The calculated Ti-Mo phase diagram according to the thermodynamic assessment of Shim et al.[16] is presented in Fig. 12, where bcc phase decomposes spinodally at low temperatures. As described in section 3.2, there is a quite large amount of data on Mo self-diffusion coefficients, but their scatter is pretty large above 2000 K. Considering that the data from Bronfin et al.,[28] Danneberg and Krautz,[29] and Maier et al.[31] show reasonable agreement over the whole temperature range, it is decided to trust only these data in the present assessment. Accordingly, a good agreement between the calculated Mo self-diffusion coefficients and such selected experimental values can be seen in Fig. 13. In Fig. 14, the calculated impurity diffusion coefficients of Mo in bcc Ti are presented, along with the data from various authors. There have been rare data reported for the impurity diffusion coefficients of Ti in bcc Mo. The results reported by Hartley et al.[36] and Thibon et al.[37] are all from interdiffusion experiments. In the assessment, higher weight is given to the result from Hartley et al.[36] and three data from Thibon

Table 2 Mobility parameters for the bcc phase in the Ti-Mo binary system (all in SI units)

Phase	Model	Mobility	Parameters
bcc	$(Ti,Mo)_1(Va)_3$	Ti	$\Phi^{Ti}_{Ti} = -151989.95 - 127.37T$[9]
			$\Phi^{Mo}_{Ti} = -435701.23 - 72.67T$
			${}^0\Phi^{Mo,Ti}_{Ti} = -91728.48 + 64.56T$
			${}^1\Phi^{Mo,Ti}_{Ti} = -96300.05$
		Mo	$\Phi^{Mo}_{Mo} = -479740.87 - 63.98T$
			$\Phi^{Ti}_{Mo} = -196255.40 - 105.21T$
			${}^0\Phi^{Mo,Ti}_{Mo} = -24153.22 - 45.32T$
			${}^1\Phi^{Mo,Ti}_{Mo} = -61804.04$

Note: Mobility parameters for self-diffusion of bcc Ti are taken from Ref 9

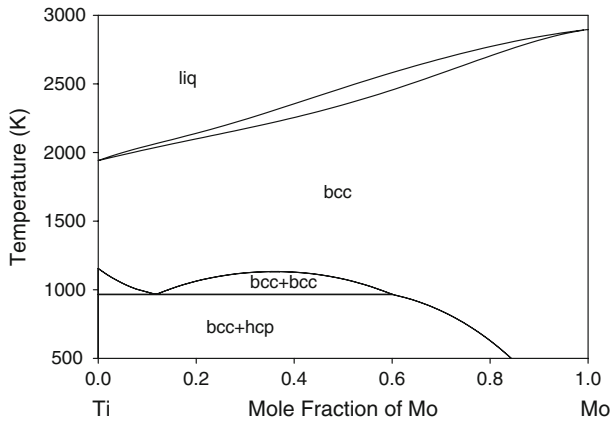

Fig. 12 Calculated Ti-Mo phase diagram according to the thermodynamic assessment of Shim et al.[16]

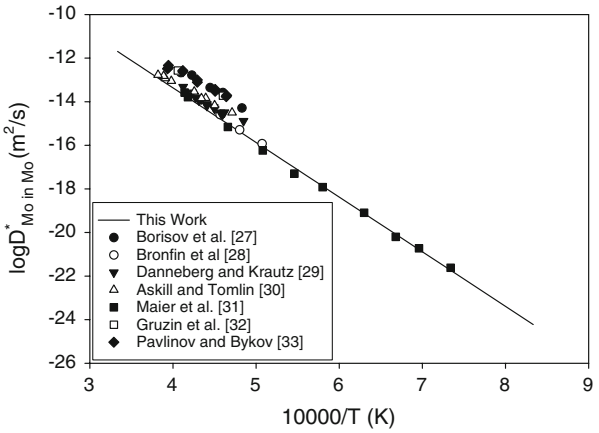

Fig. 13 Calculated and experimentally measured self-diffusion coefficients of bcc Mo

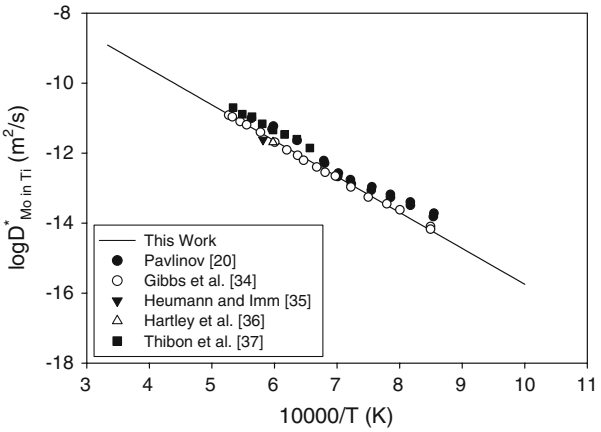

Fig. 14 Calculated and experimentally measured impurity diffusion coefficients of Mo in bcc Ti

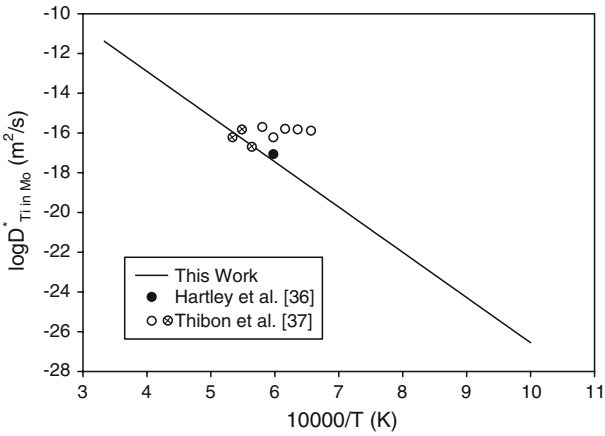

Fig. 15 Calculated and experimentally measured impurity diffusion coefficients of Ti in bcc Mo

et al.,[37] which are represented by the crossed open circles in Fig. 15, are selected to get a compromise. The obtained activation enthalpy can be justified by the value of 420000 J/mol proposed by Hartley et al.[36] In fact, the quality of mobility end-member for Ti in bcc Mo is not that significant, as Mo is an alloying element in Ti alloys. As such, one can always obtain high quality kinetic values by adjusting the interaction parameters rather than the end-member of Ti in bcc Mo itself.

The calculated intrinsic diffusion coefficients and interdiffusion coefficients at 1719 K are given in Fig. 16, together with the experimental values from Heumann and Imm.[35] As is evident, the Ti intrinsic diffusion coefficients are generally greater than the Mo intrinsic diffusion coefficients within the whole composition range at 1719 K. Moreover, the three kinds of diffusion coefficients generally increase with the Ti content. The interdiffusion coefficients measured by Hartley et al.[36] with incremental diffusion couples are plotted in Fig. 17, together with the calculated

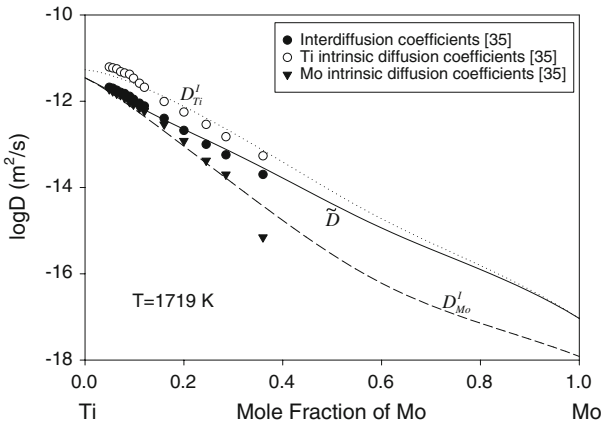

Fig. 16 Calculated and experimentally measured diffusion coefficients in bcc Ti-Mo alloys

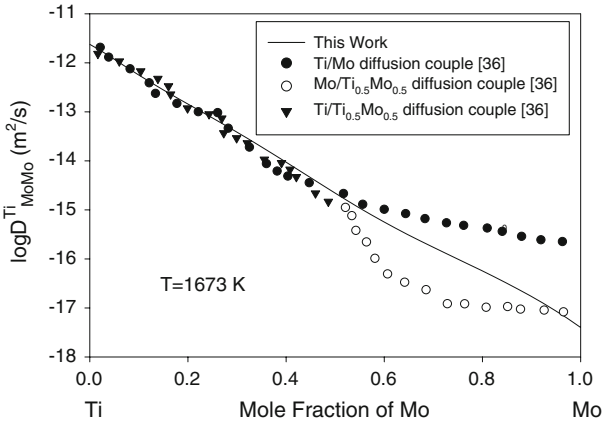

Fig. 17 Calculated and experimentally measured interdiffusion coefficients in bcc Ti-Mo alloys

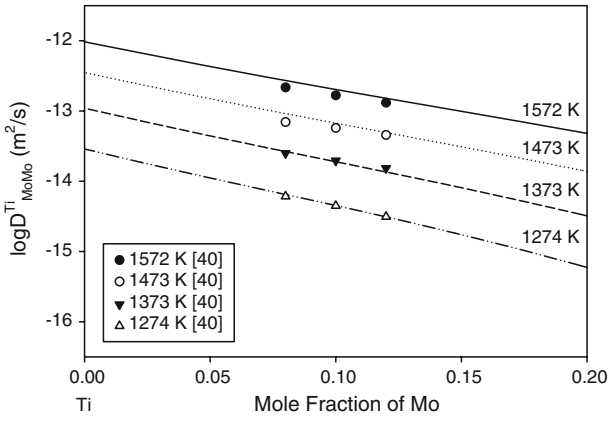

Fig. 18 Calculated and experimentally measured interdiffusion coefficients in bcc Ti-Mo alloys

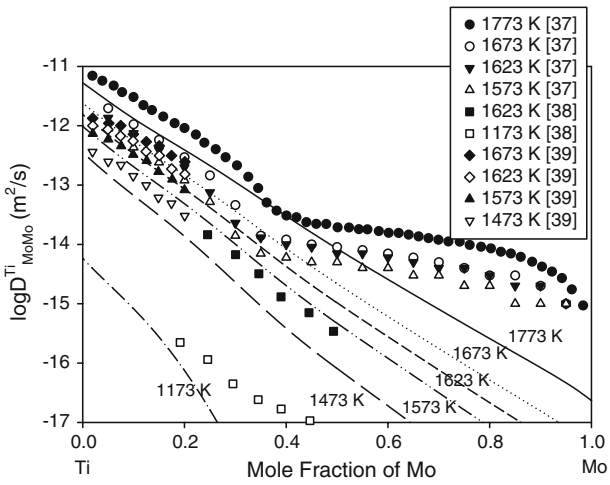

Fig. 19 Calculated and experimentally measured interdiffusion coefficients in bcc Ti-Mo alloys

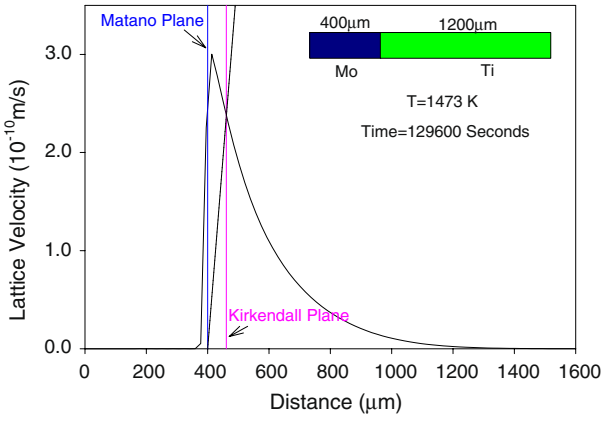

Fig. 20 Lattice velocity construction to determine Kirkendall marker displacement

values. There is a good fit near the Ti-rich edge, but a large deviation exists around the Mo-rich edge. Such a dramatic disagreement is not surprising in diffusion couples where the interdiffusion coefficients change by several magnitudes within the whole composition range. Accordingly, the concentration curves measured in diffusion couples made of pure metals will be very steep near the Mo-rich side, which will impose challenges in obtaining accurate concentration gradients to evaluate the interdiffusion coefficients. As can be seen in Fig. 17, the calculated line is a compromise near the Mo-rich edge, but the fit is good for the Ti-rich edge. The presently obtained mobility parameters also cater for the interdiffusion coefficients measured by Sprengel et al.[40] near the Ti-rich edge, as evidenced in Fig. 18. The interdiffusion coefficients measured by Thibon et al.,[37] Fedotov et al.,[38] and Majima and Isomoto[39] are presented in Fig. 19, along with the presently calculated results. The calculated results show a large deviation from the experimental data near the Mo-rich edge, which is again due to the steep concentration gradients in Ti/Mo diffusion couples around the Mo-rich side. It should also be noted that the data presented in Fig. 19 suffer from their inability in extrapolating the impurity diffusion coefficients of Mo in bcc Ti, and therefore those data are given lower weighting factors in the assessment.

When a diffusion process is governed by the vacancy mechanism, a difference in intrinsic atomic fluxes inside an interaction zone is compensated by a counter vacancy flow. Such a phenomenon can be visualized by the markers placed within the interdiffusion zone, the velocity of which can be determined from[41]:

$$\vec{u} = (D^{\mathrm{I}}_{\mathrm{Ti}} - D^{\mathrm{I}}_{\mathrm{Mo}})\nabla x_{\mathrm{Ti}} \qquad \text{(Eq 17)}$$

where $\vec{u}$ is the marker velocity. It is commonly accepted that the Kirkendall makers represent the initial contact plane moving according to the parabolic law. As such, the velocity of the Kirkendall markers is equal to[41]:

$$\vec{u}_{\mathrm{k}} = \frac{\vec{r}_{\mathrm{k}}}{2t} \qquad \text{(Eq 18)}$$

where $\vec{u}_{\mathrm{k}}$ and $\vec{r}_{\mathrm{k}}$ are the Kirkendall marker velocity and position, respectively.

Equations 17 and 18 can be used to predict the position of the Kirkendall plane, with the concentration dependence of the intrinsic diffusivities known. The position of the Kirkendall planes is located graphically as the intersection point of the velocity curve in Eq 17 and the straight line in Eq 18. The lattice velocities developed in a Ti/Mo diffusion couple annealed at 1473 K for 129600 s are plotted in Fig. 20, where the straight line from Eq 18 is also superimposed to determine the Kirkendall marker displacement from the intersection point. As is evident, the Kirkendall markers shift to the Ti-rich side due to the higher intrinsic diffusion coefficients of Ti. Such a procedure is applied to Ti/Mo diffusion couples annealed at 1673, 1573, and 1473 K for various time, and the calculated results for the Kirkendall marker displacements are compared with the results of Majima and Isomoto[39] in Fig. 21. There exist good agreements between the predicted and

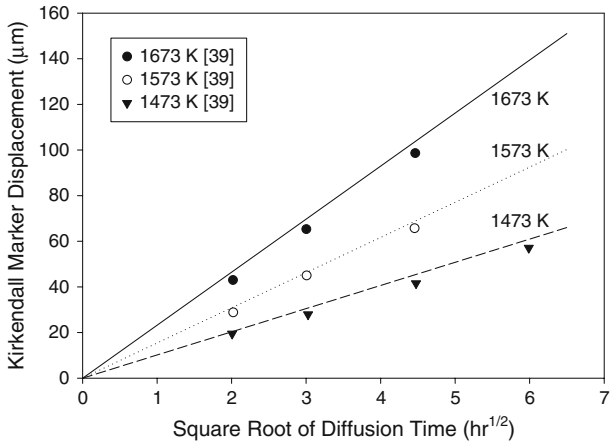

Fig. 21 Kirkendall marker displacement with respect to time and temperature

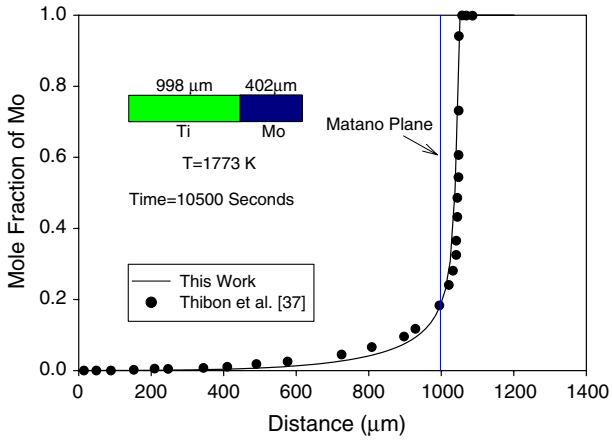

Fig. 22 Calculated and experimentally measured Mo distribution in a Ti/Mo diffusion couple

measured displacements, thereby providing an indirect evidence to verify the quality of the mobility parameters derived in this work.

The Mo concentration profile from Thibon et al.[37] is presented in Fig. 22, along with the calculated curve in this work. It is seen that the concentration curve is characterized by a long tail in the Ti-rich side and a steep concentration gradient near the Mo-rich side, which imposes a great challenge in evaluating the interdiffusion coefficients with the Boltzmann-Matano method.

5. Conclusions

Based on the various kinds of diffusion coefficients and concentration curves reported in the literature, the atomic mobilities in bcc Ti-Zr and bcc Ti-Mo alloys are critically assessed with the CALPHAD method. Comprehensive comparisons between the calculated and experimentally measured diffusion coefficients are made, where the atomic mobilities derived in this work enable most of the measured diffusivities to be reproduced. In addition, the concentration profiles of some semi-infinite diffusion couples in both binary systems and the displacements of Kirkendall makers in the Ti-Mo binary system are successfully predicted by the combination of presently obtained atomic mobility parameters and the related thermodynamic parameters in the literature.

References

1. A.K. Gogia, High-temperature Titanium Alloys, *Def. Sci. J.*, 2005, **55**(2), p 149-173
2. M. Niinomi, Recent Research and Development in Titanium Alloys for Biomedical Applications and Healthcare Goods, *Sci. Tech. Adv. Mater.*, 2003, **4**, p 445-454
3. V. Raman, S. Tamilselvi, S. Nanjundan, and N. Rajendran, Electrochemical Behavior of Titanium and Titanium Alloy in Artificial Saliva, *Trends Biomater. Artif. Organs.*, 2005, **18**(2), p 137-140
4. N.T.C. Oliveira and A.C. Guastaldi, Electrochemical Stability and Corrosion Resistance of Ti-Mo Alloys for Biomedical Applications, *Acta Biomater.*, 2009, **5**, p 399-405
5. Q. Chen, N. Ma, K. Wu, and Y. Wang, Quantitative Phase Field Modeling of Diffusion-Controlled Precipitate Growth and Dissolution in Ti-Al-V, *Scripta Mater.*, 2004, **50**, p 471-476
6. J.O. Andersson and J. Ågren, Models for Numerical Treatment of Multicomponent Diffusion in Simple Phases, *J. Appl. Phys.*, 1992, **72**(4), p 1350-1355
7. C.E. Campbell, W.J. Boettinger, and U.R. Kattner, Development of a Diffusion Mobility Database for Ni-base Superalloys, *Acta Mater.*, 2002, **50**, p 775-792
8. G. Ghosh, Thermodynamic and Kinetic Modeling of the Cr-Ti-V System, *J. Phase Equilib. Diff.*, 2002, **23**(4), p 310-328
9. Y. Liu, Y. Ge, D. Yu, T. Pan, and L. Zhang, Assessment of the Diffusional Mobilities in bcc Ti-V Alloys, *J. Alloys Comp.*, 2009, **470**(1-2), p 176-182
10. Y. Liu, T. Pan, L. Zhang, D. Yu, and Y. Ge, Kinetic Modeling of Diffusion Mobilities in bcc Ti-Nb Alloys, *J. Alloys Comp.*, 2009, **476**(1-2), p 429-435
11. J.B. Brady, Reference Frames and Diffusion Coefficients, *Am. J. Sci.*, 1975, **275**, p 954-983
12. B. Jönsson, Assessment of the Mobilities of Cr, Fe and Ni in bcc Cr-Fe-Ni Alloys, *ISIJ Int.*, 1995, **35**(11), p 1415-1421
13. T. Helander and J. Ågren, A Phenomenological Treatment of Diffusion in Al-Fe and Al-Ni Alloys Having B2-B.C.C. Ordered Structure, *Acta Mater.*, 1999, **47**(4), p 1141-1152
14. L.E. Trimble, D. Finn, and A. Cosgarea, A Mathematical Analysis of Diffusion Coefficients in Binary Systems, *Acta Metall.*, 1965, **13**, p 501-507
15. M.A. Turchanin, P.G. Agraval, and A.R. Abdulov, Thermodynamic Assessment of the Cu-Ti-Zr System. II. Cu-Zr and Ti-Zr Systems, *Powder Metall. Met. Ceram.*, 2008, **47**(7-8), p 428-446
16. J. Shim, C. Oh, and D.N. Lee, A Thermodynamic Evaluation of the Ti-Mo-C System, *Metall. Mater. Trans. B*, 1996, **27**, p 955-966
17. Y. Liu, L. Zhang, T. Pan, D. Yu, and Y. Ge, Study of Diffusion Mobilities of Nb and Zr in bcc Nb-Zr Alloys, *CALPHAD*, 2008, **32**, p 455-461
18. C.E. Campbell, A New Technique for Evaluating Diffusion Mobility Parameters, *J. Phase Equilib. Diff.*, 2005, **26**(5), p 435-440

19. W.B.J. Zimmerman, Coupling Variables Revisited: Inverse Problems, Line Integrals, Integral Equations, and Integro-differential Equations, *Multiphysics Modeling with Finite Element Methods*, W.B.J. Zimmerman, Ed., World Scientific Publishing Co., 2006, p 237-276
20. L.B. Pavlinov, Diffusion of Metal Impurities in Zirconium and Titanium, *Phys. Met. Metall.*, 1967, **24**(2), p 70-74
21. H. Araki, Y. Minamino, T. Yamane, T. Nakatsuka, and Y. Miyamoto, Pressure Dependence of Anomalous Diffusion of Zirconium in β-Titanium, *Metall. Trans. A*, 1996, **27**, p 1807-1814
22. C. Herzig, U. Köhler, and M. Büscher, Temperature Dependence of ^{44}Ti and ^{95}Zr Diffusion and of ^{88}Zr/^{95}Zr Isotope Effect in the Equiatomic BCC TiZr-Alloy, *Defect Diff. Forum*, 1993, **95-98**, p 793-798
23. I. Thibon, D. Ansel, and T. Gloriant, Interdiffusion in β-Ti-Zr Binary Alloys, *J. Alloys Comp.*, 2009, **470**(1-2), p 127-133
24. A. Brunsch and S. Steeb, Diffusion Investigation in the Ti-Zr System by Means of a Microprobe, *Z. Naturforsch. A*, 1974, **29**(9), p 1319-1324
25. V.S. Raghunathan, G.P. Tiwari, and B.D. Sharma, Chemical Diffusion in the β Phase of the Zr-Ti Alloy System, *Metall. Trans.*, 1972, **3**, p 783-788
26. K. Bhanumurthy, A. Laik, and G.B. Kale, Novel Method of Evaluation of Diffusion Coefficients in Ti-Zr System, *Defect Diff. Forum*, 2008, **279**, p 53-62
27. Y.V. Borisov, P.L. Gruzin, L.V. Pavlinov, and G.B. Fedorov, Self-Diffusion of Molybdenum, *Metall. Metalloved.*, 1959, **1**, p 213-218
28. M.B. Bronfin, S.Z. Bokshtein, and A.A. Zhukhovitsky, Self-Diffusion in Molybdenum, *Zavod. Lab.*, 1960, **26**(7), p 828-830
29. W. Danneberg and E. Krautz, Self Diffusion in Mo, *Z. Naturforsch.*, 1961, **16a**, p 854-857
30. J. Askill and D.H. Tomlin, Self Diffusion in Molybdenum, *Phil. Mag.*, 1963, **8**(90), p 997-1001
31. K. Maier, H. Mehrer, and G. Rein, Self Diffusion in Molybdenum, *Z. Metallkd.*, 1979, **70**, p 271-276
32. P.L. Gruzin, L.V. Pavlinov, and A.D. Tyutyunnik, Self-diffusion of Chromium and Molybdenum, *Izvest. Akad. Nauk SSSR Ser. Fiz.*, 1959, **5**, p 155-159
33. L.V. Pavlinov and V.N. Bykov, Self Diffusion in Molybdenum, *Fiz. Met. Metalloved.*, 1964, **18**, p 459-461
34. G.B. Gibbs, D. Graham, and D.H. Tomlin, Diffusion in Titanium and Titanium-Niobium Alloys, *Phil. Mag.*, 1963, **8**(92), p 1269-1282
35. T. Heumann and R. Imm, Study of the Kirkendall Effect in bcc Titanium-Molybdenum Alloys, *Forschungsberichte des Landes Nordrhein-Westfalen*, 1978, **2781**, p 5-25
36. C.S. Hartley, J.E. Steedly, and L.D. Parsons, Binary Interdiffusion in Body-Centered Cubic Transition Metal Systems, *Diffusion in Body-Centered Cubic Metals*, J.A. Wheeler and F.R. Winslow, Ed., American Society for Metals, 1965, p 51-75
37. I. Thibon, D. Ansel, M. Boliveau, and J. Debuigne, Interdiffusion in the β Mo-Ti Solid Solution at High Temperatures, *Z. Metallkd.*, 1998, **89**, p 187-191
38. S.G. Fedotov, M.G. Chundinov, and K.M. Konstantinov, Mutual Diffusion in the Systems Ti-V, Ti-Nb, Ti-Ta and Ti-Mo, *Fiz. Metal. Metalloved.*, 1969, **27**(5), p 873-876
39. K. Majima and T. Isomoto, Sintering Characteristics and Diffusion Process in the Titanium-Molybdenum System, *J. Jpn. Soc. Powder Metall.*, 1982, **29**(8), p 18-23
40. W. Sprengel, T. Yamada, and H. Nakajima, Interdiffusion in Binary β-Titanium Alloys, *Defect Diff. Forum*, 1997, **143-147**, p 431-436
41. M.J.H. van Dal, A.M. Gusak, C. Cserháti, A.A. Kodentsov, and F.J.J. van Loo, Spatio-temporal Instabilities of the Kirkendall Marker Planes During Interdiffusion in β'-AuZn, *Phil. Mag. A*, 2002, **82**(5), p 943-954